Chinese Journal of
POLYMER SCIENCE 高分子科学

Miscibility and Crystallization Behavior of Novel Branched Poly(ethylene succinate)/Poly(vinyl phenol) Blends

Zhang Kang-Jing, Qiu Zhao-Bin

Cite this article as:
Zhang Kang-Jing, Qiu Zhao-Bin. Miscibility and Crystallization Behavior of Novel Branched Poly(ethylene succinate)/Poly(vinyl phenol) Blends[J]. *Chinese J. Polym. Sci*, 2019, 37(11): 1169-1175. doi: 10.1007/S10118-019-2269-1

View online: https://doi.org/10.1007/S10118-019-2269-1

Chinese Journal of
POLYMER SCIENCE

ARTICLE

https://doi.org/10.1007/S10118-019-2269-1
Chinese J. Polym. Sci. **2019**, *37*, 1169–1175

Miscibility and Crystallization Behavior of Novel Branched Poly(ethylene succinate)/Poly(vinyl phenol) Blends

Kang-Jing Zhang and Zhao-Bin Qiu*

State Key Laboratory of Chemical Resource Engineering, Beijing University of Chemical Technology, Beijing 100029, China

Abstract The blends of novel branched poly(ethylene succinate) (b-PES) and poly(vinyl phenol) (PVPh) were prepared *via* a solution and casting method. The miscibility, melting behavior, spherulitic morphology and growth, and crystal structure of b-PES/PVPh blends were investigated in detail. PVPh was miscible with b-PES over the whole compositions as evidenced by the single composition dependent glass transition temperature. Double melting behavior occurred in neat b-PES and b-PES/PVPh 85/15 blend after isothermal melt crystallization, which may be explained by the melting, recrystallization, and remelting mechanism. In addition, the depression of equilibrium melting point of an 85/15 blend was also found, confirming again the miscibility between the two components. The addition of PVPh caused the decrease of nucleation density and crystal growth rates of b-PES spherulites in the blend. The crystal structure of b-PES was unchanged before and after blending; moreover, the crystallinity of b-PES decreased slightly in the blend.

Keywords Polymer blends; Miscibility; Crystallization behavior

Citation: Zhang, K. J.; Qiu, Z. B. Miscibility and crystallization behavior of novel branched poly(ethylene succinate)/poly(vinyl phenol) blends. *Chinese J. Polym. Sci.* **2019**, *37*, 1169–1175.

INTRODUCTION

Traditional polymer products from fossil resources have brought serious white pollution and plastic waste due to the nondegradable nature. As a member of biodegradable and biocompatible polymers, poly(ethylene succinate) (PES) has drawn considerable attention in the field of environmentally friendly materials. PES is able to degrade completely under simple conditions; moreover, its monomer, succinic acid, can be derived from natural resources. Many studies have reported the melting behavior, crystallization kinetics, morphology, and crystal structure of PES.[1–6] In addition, some PES-based polymer blends have been prepared to modify the physical properties for extending the practical applications.[7–10] Although blending is an efficient way to improve the properties of polymeric materials, it may face the fact of phase separation, which may not meet the practical requirement.[11,12] In addition to physical polymer blends, copolymerization is also an effective chemical method to modify the properties of PES by changing the structure units of molecular chain. Many researchers have extensively reported the crystalline morphology, crystallization kinetics, mechanical properties, crystal structure, and degradation behaviors of PES-based copolymers, such as poly(ethylene succinate-*co*-propylene succinate), poly(ethylene succinate-*co*-butylene succinate), poly(ethylene succinate-*co*-octamethylene succinate), poly(ethylene succinate-*co*-decamethylene succinate), poly(ethylene succinate-*co*-ethylene adipate), and poly(ethylene succinate-*co*-ethylene suberate).[13–20] In general, these PES-based copolymers are linear aliphatic polyesters. However, novel branched polymers have opened a new way in modification by introducing side chains, which may decrease glass transition temperature and melting temperature.[21–25] In our previous work, two novel branched and random PES copolymers containing 4.6 mol% and 9.6 mol% *n*-octyl pendant group as side chains were synthesized through copolymerization with the comonomer of 1,2-decanediol. The glass transition temperature, melting point, dynamic storage modulus values, and heat of fusion of branched PES copolymers were lower than those of linear PES and decreased gradually with increasing side chains content. The branched PES copolymers behaved as non-Newtonian fluid and had the same crystal structures as linear PES, but degraded slower in the alkaline environment than linear PES.[26]

Poly(vinyl phenol) (PVPh), as a proton donor, offers excellent potential for hydrogen-bonding interactions with proton acceptor polymers. PVPh is an amorphous polymer with high glass transition temperature. Many researchers have reported that PVPh is miscible with various polymers, such as poly(ε-caprolactone) (PCL), poly(L-lactide) (PLLA), poly(butylene succinate) (PBS), poly(ethylene succinate) (PES)poly(butylenesuccinate-*co*-butyleneadipate)(PBSA)poly-(3-hydroxybutyrate-*co*-3-hydroxyhexanoate) (PHBHHx), poly(butylene succinate-*co*-butylene carbonate) (PBSC), poly(butylene suberate) (PBSub), and poly(ethylene oxide)

* Corresponding author: E-mail qiuzb@mail.buct.edu.cn

Received March 11, 2019; Accepted April 4, 2019; Published online May 24, 2019

(PEO).[27–35] These polyesters all have carbonyl groups, which can form hydrogen bonding interaction with the hydroxyl groups of PVPh, leading to the miscibility of these polymer blends.

From the specific molecular interaction viewpoint of the two components, b-PES may form novel miscible polymer blends with PVPh. However, b-PES/PVPh blends have not been reported so far. Therefore, the miscibility, melting behavior, morphology, and crystal structure of the novel crystalline/amorphous polymer blends were investigated in this work. The research values and novelties of this research are as follows. First, the miscibility, melting behavior, and morphology of b-PES/PVPh blends were studied for the first time to better understand the miscible crystalline/amorphous blends with specific interaction. Second, this research should be the first study on novel b-PES-based polymer blends. Third, as a new polyester, the potential application with desired properties of b-PES may be extended by polymer blending from a practical viewpoint. This work should be an important and interesting study on the miscibility and crystallization behavior of biodegradable polymer blends, especially in branched polymer/PVPh blending systems.

EXPERIMENTAL

Materials and Preparation of b-PES/PVPh Blends

PVPh (M_w = 1.1 × 10^4 g/mol) was purchased from Sigma-Aldrich (Shanghai) Trading Co., Ltd. The branched and random PES (M_w = 8.8 × 10^4 g/mol, M_n = 5.9 × 10^4 g/mol) containing 5 mol% 1,2-decamethylene succinate (DS) unit was synthesized by our laboratory *via* a typical two-stage (including esterification and polycondensation) melt condensation method by using ethylene glycol, succinic acid, and 1,2-decanediol as the monomers (the molar feed ratio of ethylene glycol/1,2-decanediol = 95/5) and tetrabutyl titanate as the catalyst. The detailed preparation procedure is described elsewhere and not shown here for brevity.[26] *N*,*N*-dimethylformamide (DMF) was used as a mutual solvent. Fig. 1 displays the chemical structures of b-PES and PVPh.

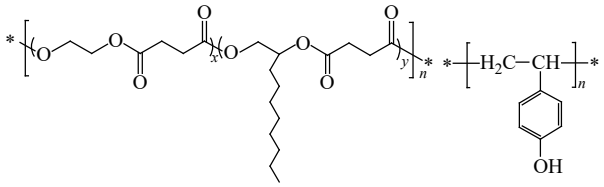

Fig. 1 Chemical structures of b-PES (left) and PVPh (right)

Neat and blended b-PES were prepared *via* a solution and casting method. The preparation of b-PES/PVPh blends was described as follows. First, b-PES/PVPh blends with various weight ratios of 85/15, 70/30, 50/50, 30/70, and 15/85 were dissolved in DMF at 50 °C through a continuous magnetic stirring for 4 h. Second, the solutions were poured into petri dishes to evaporate the solvent at room temperature for 24 h. Third, the blend films were further transferred into a vacuum oven at 50 °C for 72 h to remove the residual solvent completely. The blends with different weight ratios of the two components were abbreviated as 85/15, 70/30, 50/50, 30/70, and 15/85, respectively. In addition, neat b-PES film was prepared in a similar way.

Characterization

The miscibility and melting behaviors of neat and blended b-PES were studied by using a TA instruments Q100 differential scanning calorimeter (DSC) with a Universal Analysis 2000 software under nitrogen atmosphere. Each fresh sample was around 4 mg. The samples were first heated to 190 °C and held there for 3 min to erase any previous thermal history. For the glass transition temperature (T_g) measurement, neat and blended b-PES were quenched to −40 °C from the crystal-free melt at 60 °C/min, and the subsequent DSC heating traces were recorded at 20 °C/min. For the melting behavior study, the samples were cooled to the chosen crystallization temperature at 40 °C/min, maintained for 1 h to ensure complete crystallization, and heated again at 20 °C/min to study the subsequent melting behavior. It should be emphasized that only the melting behavior of neat b-PES and 85/15 blend was studied in this research, because other samples crystallized too slow or even did not crystallize when the weight fraction of PVPh was higher than 30% in the blends.

The spherulitic morphology of neat and blended b-PES was investigated with a polarizing optical microscope (POM) (Olympus BX51) equipped with a Linkam THMS 600 hot stage. The samples were cooled at 60 °C/min to isothermal crystallization temperature from the crystal-free melt after erasing any thermal history.

The crystal structures of neat and blended b-PES were studied with a Rigaku D/Max 2500 VB2t/PC X-ray diffractometer at 40 kV and 200 mA using a speed of 5 (°)/min from 5° to 45° at room temperature. The samples for the wide angle X-ray diffraction (WAXD) experiments were first pressed into films of about 1 mm in thickness from the crystal-free melt on a hot stage at 130 °C and then transferred into a vacuum oven at 65 °C for 72 h.

RESULTS AND DISCUSSION

Miscibility Study of b-PES/PVPh Blends

It is one of the most efficient methods to evaluate the miscibility of polymer blends through the T_g study, when the difference in T_gs of the two neat components is over 20 °C. If they are miscible, only one single composition dependent T_g will exist between those of the two neat components. If they are partially miscible or immiscible, two T_gs from the two components will be detected. The miscibility of binary crystalline/amorphous b-PES/PVPh blends was first studied with DSC. Fig. 2 shows the DSC thermograms of neat b-PES, neat PVPh, and their blends with different compositions. As introduced in the experimental part, all samples were quenched from the melt state, and the T_g values were measured at a heating rate of 20 °C/min from the amorphous state. Neat b-PES showed the lowest T_g of −10.9 °C, while neat PVPh had the highest one of 170.7 °C. The difference in T_g between b-PES and PVPh was about 180 °C. The b-PES/PVPh

https://doi.org/10.1007/S10118-019-2269-1

blends had a single composition dependent T_g between those of the two neat components, which increased with the increase of PVPh content, indicating that b-PES/PVPh blends were miscible. The hydrogen bonding interaction between the hydroxyl groups of PVPh and the carbonyl groups of b-PES should be responsible for the good miscibility of b-PES/PVPh blends, which will need further investigation in the forthcoming research. Neat b-PES showed an obvious melting peak at about 95.4 °C, which slightly shifted downward to 94.9 °C in the 85/15 blend and could not be detected for the other samples with high PVPh compositions. This phenomenon indicated that the crystallization of b-PES was restrained by the dilution of amorphous PVPh, especially at high PVPh content in the blends.

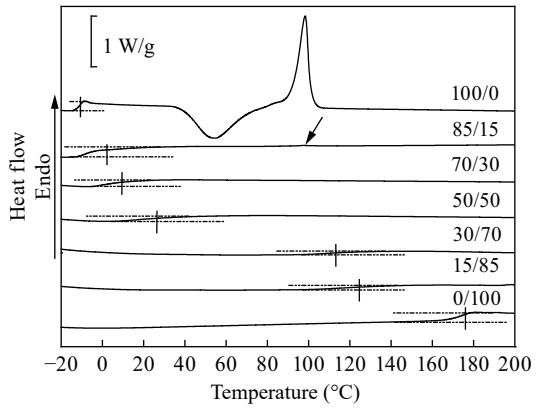

Fig. 2 The T_g measurement of b-PES/PVPh blends with DSC at a heating rate of 20 °C/min from the amorphous state (The arrow shows the melting peak of the 85/15 blend.)

The dependence of T_g on the weight fraction in PVPh in b-PES/PVPh blends is shown in Fig. 3. The solid line in Fig. 3 is based on the Fox equation, which has often been used to predict the variation of T_g of miscible blends with the blend composition:

$$\frac{1}{T_g} = \frac{W_1}{T_{g1}} + \frac{W_2}{T_{g2}} \quad (1)$$

where T_{g1} and T_{g2} are the respective T_gs, and W_1 and W_2 are the weight fractions of the neat components, respectively.[36]

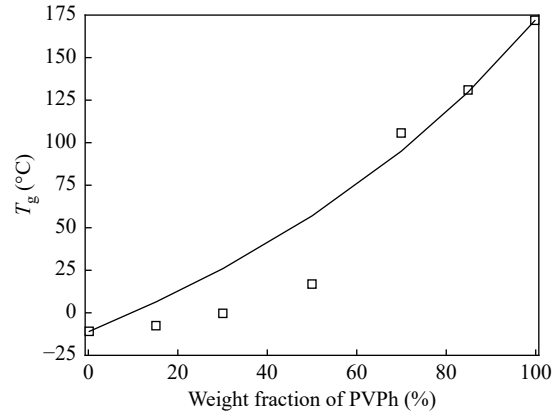

Fig. 3 Variation of T_g with the weight fraction of PVPh for b-PES/PVPh blends (The solid line is based on the Fox equation.)

Fig. 3 clearly demonstrates that T_g of the blends increased with the increasing weight fraction of PVPh; however, the increased T_g showed different blend composition dependence. When the weight fraction of PVPh was lower than 50%, T_g of the blends increased slightly from −10.9 °C for neat b-PES to 16.6 °C for 50/50 blend. In addition, the measured T_g values were all lower than those predicted by the Fox equation, indicating a negative deviation. This kind of deviation implies that the hydrogen bond interaction between the carbonyl of b-PES and the hydroxyl of PVPh may be rather weak. When the weight fraction of PVPh was higher than 70%, T_g of the blends increased abruptly from 16.6 °C for 50/50 blend to 104.9 °C for 30/70 blend. By merely increasing the weight fraction of PVPh from 50% to 70%, the increase in T_g was almost 90 °C. In addition, the measured T_g values were very close to those fitted by the Fox equation when the weight fraction of PVPh was higher than 70%. The blend composition played an important role in affecting the T_g values of b-PES/PVPh blends, which may arise from the different hydrogen bond interaction strengths between components within different blend composition ranges. When the weight fraction of PVPh was 70% and above, the interaction was strong, and the T_g values of the blends were well fitted by the Fox equation. On the other hand, when the weight fraction of PVPh was 50% and below, the measured T_g values of the blends were lower than those predicted by the Fox equation because of the weak interaction. The strong interaction would lead to high T_g values, while the weak interaction would lead to low T_g values. Such phenomenon was also reported in PHBHHx/PVPh blends.[32] The dependence of T_g values on blend compositions is common in blending systems. Penning *et al*. once reported that the T_g values of poly(vinylidene fluoride)/poly(1,4-butylene adipate) (PVF_2/PBA) blends displayed a sigmoidal curve with composition.[37] In brief, the deviation of T_g values was dominated by the more abundant blend component.

Melting Behavior and Equilibrium Melting Point Study of b-PES/PVPh Blends

In addition to the single composition dependent T_g, the depression of the equilibrium melting point temperature of crystalline component is another powerful evidence of miscibility with amorphous component in miscible crystalline/amorphous polymer blends.[38,39] Therefore, the melting behavior of neat and blended b-PES was studied in this section to determine the equilibrium melting point temperatures.

Fig. 4 displays the subsequent melting behavior of an 85/15 blend after crystallizing at various T_cs for 1 h, from which two melting endothermic peaks were observed. The lower melting peak temperature (T_{m1}) shifted upward to a higher temperature with increasing T_c, while the higher melting peak temperature (T_{m2}) was almost unchanged. As shown in Fig. 4, T_{m1} increased gradually from 80 °C to 85.5 °C, while T_{m2} was maintained at about 95 °C. Similar phenomenon also occurred in neat b-PES. The ratio of the area of T_{m1} to that of T_{m2} increased with increasing T_c; moreover, the two melting peaks were found to approach each other gradually. Such double melting behavior may be explained by the melting, recrystallization, and remelting mechani-

https://doi.org/10.1007/S10118-019-2269-1

sm.[40–42] According to this mechanism, T_{m1} was the melting point of the crystals formed at T_c during isothermal crystallization prior to the heating scan in DSC, while T_{m2} was originated from the melting of the crystals formed through recrystallization at T_c in the subsequent heating process.

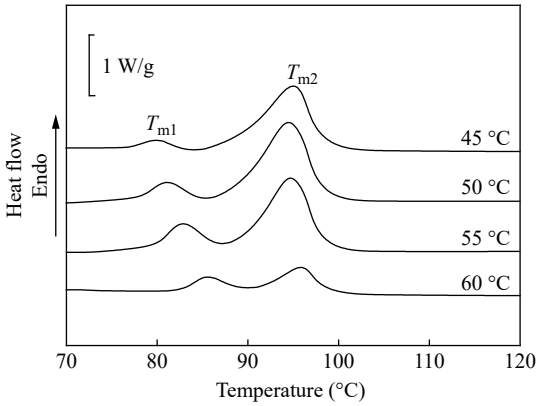

Fig. 4 Subsequent melting behavior of 85/15 blend at heating rate of 20 °C/min after crystallizing at indicated T_c values for 1 h

To confirm the mechanism proposed above, the heating rate dependence of the double melting behavior of an 85/15 blend was further investigated with DSC. Fig. 5 illustrates the double melting behavior of the 85/15 blend at different heating rates from 5 °C/min to 20 °C/min after crystallizing at 55 °C for 1 h. As clearly shown in Fig. 5, T_{m1} increased while T_{m2} decreased with the increasing heating rate. In addition, the ratio of the area of T_{m1} to that of T_{m2} became greater with the increasing heating rate. In other words, the recrystallization was restricted with the increasing heating rate. The results shown in Figs. 4 and 5 indicate that the double melting behavior of neat and blended b-PES should be attributed to the melting, recrystallization, and remelting processes; therefore, T_{m1} was used for the estimation of equilibrium melting point.

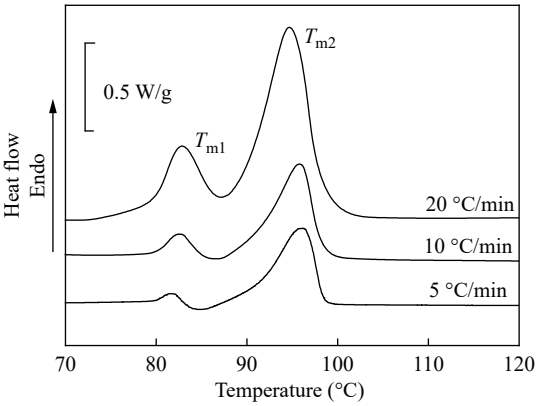

Fig. 5 Heating rate dependence of double melting behavior of an 85/15 blend after crystallizing at 55 °C for 1 h

Hoffman and Weeks proposed the following relationship between apparent melting point (T_m) and T_c:

$$T_m = \eta T_c + (1 - T_c) T_m^{o} \quad (2)$$

where T_m^{o} is the equilibrium melting point, and η can be regarded as a measure of the stability, *i.e.*, the lamellar thickness, of the crystals undergoing the melting process.[43]

Fig. 6 displays the Hoffman-Weeks plot for the estimation of T_m^{o} of an 85/15 blend. From Fig. 6, T_m^{o} was determined to be 99.5 °C for 85/15 blend. Similarly, T_m^{o} was found to be 102.9 °C for neat b-PES. For simplicity, the Hoffman-Weeks plot for the estimation of T_m^{o} of neat b-PES was omitted. T_m^{o} of 85/15 blend was lower than that of neat b-PES. The depression in T_m^{o} of the 85/15 blend confirmed again the good miscibility between crystalline b-PES and amorphous PVPh.[39] Similar results have also been reported for some other miscible crystalline/amorphous polymer blends.[27–32]

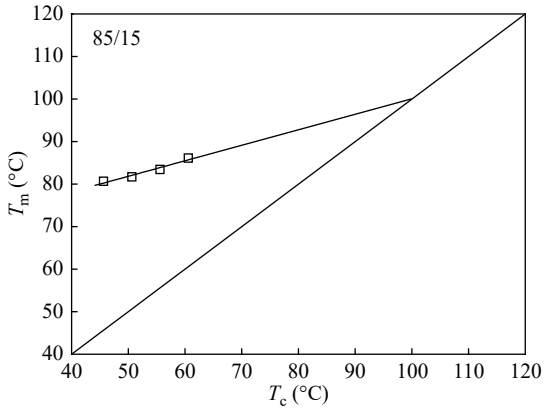

Fig. 6 Hoffman-Weeks plot for the estimation of equilibrium melting point of an 85/15 blend

Spherulites Morphology and Growth Rates of Neat and Blended b-PES

In the above sections, the miscibility, double melting behavior, and equilibrium melting point temperature of b-PES/PVPh blends were studied by DSC in detail. As spherulitic morphology and growth may influence the physical properties and biodegradation, they were further investigated with POM for neat and blended b-PES in this section. Fig. 7 presents the POM images of neat and blended PES after crystallizing at 50 °C and filling the whole space.

As displayed in Fig. 7, both neat b-PES and its blend could form regular spherulites with typical Maltese-cross feature. From the POM micrographs, the average radius was around 50 and 100 μm for neat and blended b-PES spherulites, respectively. The size of spherulites became larger by blending with 15% of PVPh at the same crystallization temperature. The decrease of nucleation density of spherulites indicated that the crystallization of b-PES was diluted by amorphous PVPh in the blend. Fig. 7 shows that the spherulites continued growing until they collided with each other and finally filled all the space, suggesting that PVPh component was expelled into the interlamellar and interfibrillar regions of b-PES spherulites.

The growth rates were further studied by measuring the radius of spherulites with crystallization time for neat b-PES and 85/15 blend at various T_c values and are shown in Fig. 8. Both the samples exhibited bell shape curves for the growth

https://doi.org/10.1007/S10118-019-2269-1

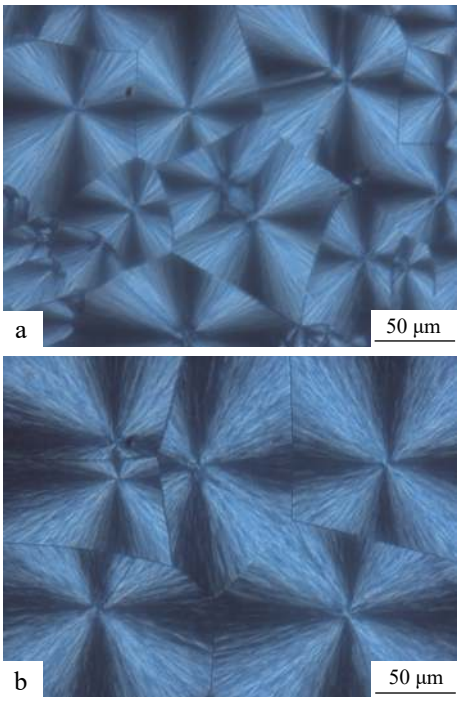

Fig. 7 Spherulites of (a) 100/0 and (b) 85/15 samples after crystallizing at 50 °C and filling the whole space

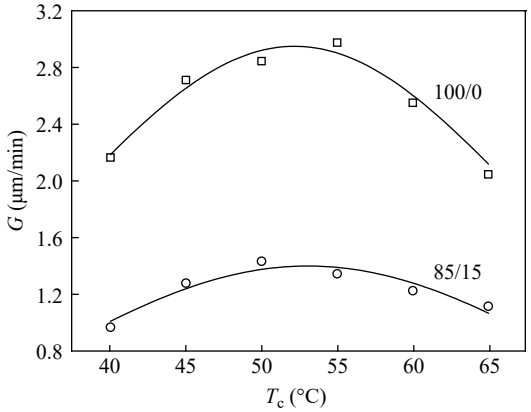

Fig. 8 Plots of G with T_c for neat and blended b-PES

rates in the T_c range of 40 °C to 65 °C. With increasing T_c, the G values of neat and blended b-PES first increased and then decreased after they reached the maximum. From Fig. 8, the spherulites of neat b-PES grew faster than those of its blend at the same T_c. For instance, the G values were 2.92 and 1.42 μm/min for neat b-PES and 85/15 blend, respectively, at T_c of 50 °C. The spherulitic growth rate of the 85/15 blend was significantly lower than that of neat b-PES. The reduction in G values of the blend may be related to the following factors: the restricted mobility of b-PES polymer chains after blending with the high T_g PVPh component, the weaker thermodynamic driving force for the growth of spherulites caused by the depression of equilibrium melting temperature, and the dilution of amorphous PVPh content in the blend. In brief, both the aforementioned DSC and POM results revealed that blending with PVPh reduced the crystallization ability of b-PES in the 85/15 blend.

Crystal Structure Study of Neat and Blended b-PES

WAXD experiments were carried out to further study the crystal structures of neat b-PES and its blend. Fig. 9 shows the WAXD patterns of neat b-PES and 85/15 blend, which were isothermally crystallized at 65 °C for 72 h. As shown in Fig. 9, both neat and blended b-PES exhibited almost the same diffraction peaks at nearly the same locations; moreover, two main diffraction peaks were observed at 2θ of around 20.1° and 23.2°, corresponding to the (021) and (200) planes of b-PES, respectively.[26] This result indicated that blending with amorphous PVPh did not modify the crystal structure of b-PES. In addition, the crystallinity values were about 36% for neat b-PES and 28% for 85/15 blend on the basis of the WAXD patterns, suggesting that blending with amorphous slightly decreased the crystallinity of b-PES.

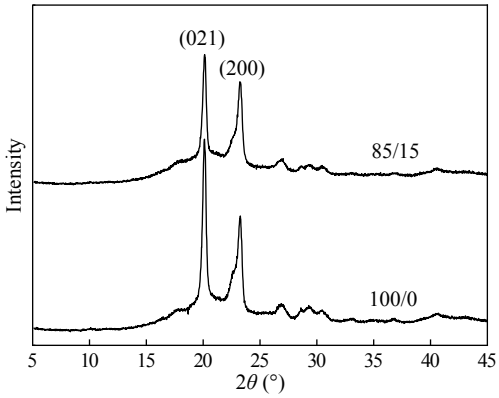

Fig. 9 WAXD patterns of neat and blended b-PES crystallized at 65 °C for 72 h

CONCLUSIONS

In this work, novel degradable branched PES/PVPh blends were prepared through a solution and casting method. The miscibility, melting behavior, spherulitic morphology and growth, and crystal structure of b-PES/PVPh blends were investigated by DSC, POM, and WAXD in detail. Crystalline b-PES was found to be miscible with amorphous PVPh over the entire compositions as evidenced by the single composition dependent glass transition temperature. The depression of the equilibrium melting point of 85/15 blend was another evidence to further support the miscibility of the two components. Double melting behavior was found for both neat b-PES and 85/15 blend after they finished the isothermal crystallization from the melt, which may be explained by the melting, recrystallization, and remelting mechanism. Through the Hoffman-Weeks equation, the equilibrium melting point temperatures of neat and blended b-PES were determined. The depression of the equilibrium melting point temperature in the blend confirmed again the miscibility between the two components. The spherulitic morphology and growth rates of neat and blended b-PES were studied with POM in a wide crystallization temperature range. The size of the spherulites of 85/15 blend became larger than that of neat b-PES, indicative of a decrease in the nucleation density. Moreover, the spherulitic growth rate of 85/15 blend

https://doi.org/10.1007/S10118-019-2269-1

was lower than that of neat b-PES at the same crystallization temperature. The reduction of spherulitic growth rate of the blend was attributed to its increased glass transition temperature, decreased equilibrium melting point temperature, and the dilution effect of amorphous component. The WAXD results illustrated that the crystal structure of b-PES was not modified by blending with PVPh, and the crystallinity decreased slightly after crystallized at 65 °C for 72 h, as revealed by the WAXD measurement.

ACKNOWLEDGMENTS

This work was financially supported by the National Natural Science Foundation of China (No. 51573016).

REFERENCES

1 Zeng, J.; Wu, F.; Huang, C.; He, Y.; Wang, Y. Urethane ionic groups induced rapid crystallization of biodegradable poly(ethylene succinate). *ACS Macro Lett.* **2012**, *1*, 965−968.
2 Tezuka, Y.; Ishii, N.; Kasuya, K.; Mitomo, H. Degradation of poly(ethylene succinate) by mesophilic bacteria. *Polym. Degrad. Stab.* **2004**, *84*, 115−121.
3 Gan, Z.; Abe, H.; Doi, Y. Biodegradable poly(ethylene succinate) (PES). 2. Crystal morphology of melt-crystallized ultrathin film and its change after enzymatic degradation. *Biomacromolecules* **2000**, *1*, 713−720.
4 Qiu, Z.; Fujinnami, S.; Komura, M.; Nakajima, K.; Ikehara, T.; Nishi, T. Nonisothermal crystallization kinetics of poly(butylene succinate) and poly(ethylene succinate). *Polym. J.* **2004**, *36*, 642−646.
5 Gan, Z.; Abe, H.; Doi, Y. Biodegradable poly(ethylene succinate) (PES). 1. Crystal growth kinetics and morphology. *Biomacromolecules* **2000**, *1*, 704−712.
6 Qiu, Z.; Komura, M.; Ikehara, T.; Nishi, T. DSC and TMDSC study of melting behavior of poly(butylene succinate) and poly(ethylene succinate). *Polymer* **2003**, *44*, 7781−7785.
7 Kataoka, T.; Abe, T.; Ikehara, T. Crystalline layered morphology in the phase-separated blend of poly(butylene succinate) and poly(ethylene succinate). *Polym. J.* **2015**, *47*, 645−648.
8 Liu, X.; Zhu, J.; Ni, H.; Chen, S. Influence of blend composition on crystallization of poly(L-lactic acid)/poly(ethylene oxide) crystalline/crystalline blends. *J. Macromol. Sci.* **2015**, *54*, 203−241.
9 Zeng, J.; Zhu, Q.; Li, Y.; Qiu, Z.; Wang, Y. Unique crystalline/crystalline polymer blends of poly(ethylene succinate) and poly(*p*-dioxanone): Miscibility and crystallization behaviors. *J. Phys. Chem. B* **2010**, *114*, 14827−14833.
10 He, Y.; Zeng, J.; Li, S.; Wang, Y. Crystallization behavior of partially miscible biodegradable poly(butylene succinate)/poly(ethylene succinate) blends. *Thermochim. Acta* **2012**, *529*, 80−86.
11 Kataoka, T.; Hiramoto, K.; Kurihara, H.; Ikehara, T. Effects of melt annealing on the miscibility and crystallization of poly(butylene succinate)/poly(ethylene succinate) blends. *Polym. J.* **2014**, *46*, 405−411.
12 Lu, J.; Qiu, Z.; Yang, W. Fully biodegradable blends of poly(L-lactide) and poly(ethylene succinate): Miscibility, crystallization, and mechanical properties. *Polymer* **2007**, *48*, 4196−4204.
13 Papageorgiou, G.; Bikiaris, D. Synthesis and properties of novel biodegradable/biocompatible poly[propylene-*co*-(ethylene succinate)] random copolyesters. *Macromol. Chem. Phys.* **2009**, *210*, 1408−1421.
14 Chen, M.; Chang, W.; Lu, H.; Chen, C.; Peng, J.; Tsai, C. Characterization, crystallization kinetics and melting behavior of poly(ethylene succinate) copolyester containing 5 mol% trimethylene succinate. *Polymer* **2007**, *48*, 5408−5416.
15 Chen, C.; Lu, H.; Chen, M.; Peng, J.; Tsai, C.; Yang, C. Synthesis and characterization of poly(ethylene succinate) and its copolyesters containing minor amounts of butylene succinate. *J. Appl. Polym. Sci.* **2009**, *111*, 14333−1439.
16 Yang, Y.; Qiu, Z. Crystallization and melting behavior of biodegradable poly(ethylene succinate-*co*-6 mol% butylene succinate). *J. Appl. Polym. Sci.* **2011**, *122*, 105−111.
17 Li, X.; Qiu, Z. Crystallization kinetics, morphology, and mechanical properties of novel poly(ethylene succinate-*co*-octamethylene succinate). *Polym. Test.* **2015**, *48*, 125−132.
18 Li, X.; Qiu, Z. Synthesis and properties of novel poly(ethylene succinate-*co*-decamethylene succinate) copolymers. *RSC Adv.* **2015**, *5*, 103713−103721.
19 Wu, H.; Qiu, Z. Synthesis, crystallization kinetics and morphology of novel poly(ethylene succinate-*co*-ethylene adipate) copolymers. *CrystEngComm* **2012**, *14*, 3586−3595.
20 Qiu, S.; Su, Z.; Qiu, Z. Crystallization kinetics, morphology and mechanical properties of novel biodegradable poly(ethylene succinate-*co*-ethylene suberate) copolyesters. *Ind. Eng. Chem. Res.* **2016**, *55*, 10286−10293.
21 Jin, H.; Kim, D.; Kim, M.; Lee, I.; Lee, H.; Yoon, J. Synthesis and properties of poly(butylene succinate) with *n*-hexenyl side branches. *J. Appl. Polym. Sci.* **2001**, *81*, 2219−2226.
22 Yan, D.; Wang, W.; Zhu, S. Effect of long chain branching on rheological properties of metallocene polyethylene. *Polymer* **1999**, *40*, 1737−1744.
23 Gao, R.; He, X.; Shao, Y.; Hu, Y.; Zhang, H.; Liu, Z.; Liu, B. Effects of branch content and branch length on polyethylene crystallization: Molecular dynamics simulation. *Macromol. Theor. Simul.* **2016**, *25*, 303−311.
24 Zheng, Y.; Tee, H.; Wei, Y.; Wu, X.; Mezger, M.; Yan, S.; Landfester, K.; Wagener, K.; Wurm, F.; Lieberwirth, I. Morphology and thermal properties of precision polymers: The crystallization of butyl branched polyethylene and polyphosphoesters. *Macromolecules* **2016**, *49*, 1321−1330.
25 Marie, V.; Nicolas, J.; Rene, S.; Nadege, B.; Christian, C.; Alain, R.; Francoise, F. Synthesis of branched poly(butylene succinate): Structure properties relationship. *Chinese J. Polym. Sci.* **2016**, *34*, 873−888.
26 Qiu, S.; Zhang, K.; Su, Z.; Qiu, Z. Thermal behavior, mechanical and rheological properties, and hydrolytic degradation of novel branched biodegradable poly(ethylene succinate) copolymers. *Polym. Test.* **2018**, *66*, 64−69.
27 Kuo, S.; Huang, C.; Chang, F. Study of hydrogen-bonding strength in poly(ε-caprolactone) blends by DSC and FTIR. *J. Polym. Sci., Part B: Polym. Phys.* **2001**, *39*, 1348−1359.
28 Zhang, L.; Goh, S.; Lee, S. Miscibility and crystallization behaviour of poly(L-lactide)/poly(*p*-vinyl phenol) blends. *Polymer* **1998**, *39*, 4841−4847.
29 Qiu, Z.; Komura, M.; Ikehara, T.; Nishi, T. Poly(butylene succinate)/poly(vinyl phenol) blends. Part 1. Miscibility and crystallization. *Polymer* **2003**, *44*, 8111−8117.
30 Qiu, Z.; Fujinami, S.; Komura, M.; Nakajima, K.; Ikehara, T.; Nishi, T. Miscibility and crystallization of poly(ethylene succinate)/poly(vinyl phenol) blends. *Polymer* **2004**, *45*, 4515−4521.
31 Yang, F.; Qiu, Z.; Yang, W. Miscibility and crystallization of

biodegradable poly(butylene succinate-*co*-butylene adipate)/poly(vinyl phenol) blends. *Polymer* **2009**, *50*, 2328−2333.
32 Cai, H.; Yu, J.; Qiu, Z. Miscibility and crystallization of biodegradable poly(3-hydroxybutyrate-*co*-3-hydroxyhexanoate)/poly(vinyl phenol) blends. *Polym. Eng. Sci.* **2012**, *52*, 233−241.
33 Weng, M.; Qiu, Z. Crystallization kinetics and morphology of novel miscible crystalline/amorphous polymer blends of biodegradable poly(butylene succinate-*co*-butylene carbonate) and poly(vinyl phenol). *Ind. Eng. Chem. Res.* **2013**, *52*, 10198−10205.
34 Shi, X.; Qiu, Z. Miscibility, crystallization behavior and morphology of novel poly(butylene suberate) and poly(vinyl phenol) blends. *RSC Adv.* **2015**, *5*, 79691−79698.
35 Hou, Y.; Wu, Q.; Chen, T.; Sun, P. Unique evolution of spatial and dynamic heterogeneities on the glass transition behavior of PVPh/PEO blends. *Chinese J. Polym. Sci.* **2012**, *30*, 900−915.
36 Fox, T. Influence of diluent and copolymer composition on the glass transition temperature of a polymer system. *Bull. Am. Phys. Soc.* **1956**, *1*, 123.
37 Penning, J.; Manley, R. Miscible blends of two crystalline polymers. 1. Phase behavior and miscibility in blends of poly(vinylidene fluoride) and poly(1,4-butylene adipate). *Macromolecules* **1996**, *29*, 77−83.
38 Flory, P. *Principles of polymer chemistry*. Cornell University Press, Ithaca, NY, **1953**.
39 Nishi, T.; Wang, T. Melting point depression and kinetic effects of cooling on crystallization in poly(vinylidene fluoride)-poly(methyl methacrylate) mixtures. *Macromolecules* **1975**, *8*, 909−915.
40 Liu, T.; Petermann, J. Multiple melting behavior in isothermally cold-crystallized isotactic polystyrene. *Polymer* **2001**, *42*, 6453−6461.
41 Qiu, Z.; Ikehara, T.; Nishi, T. Melting behaviour of poly(butylene succinate) in miscible blends with poly(ethylene oxide). *Polymer* **2003**, *44*, 3095−3099.
42 Wu, H.; Qiu, Z. A comparative study of crystallization, melting behavior, and morphology of biodegradable poly(ethylene adipate) and poly(ethylene adipate-*co*-5 mol% ethylene succinate). *Ind. Eng. Chem. Res.* **2012**, *51*, 13323−13328.
43 Hoffman, J.; Weeks, J. X-ray study of isothermal thickening of lamellae in bulk polyethylene at the crystallization temperature. *J. Chem. Phys.* **1965**, *42*, 4301−4302.

https://doi.org/10.1007/S10118-019-2269-1